

Enhanced exploration for primordial black holes using pulsar timing arrays

Kazumi. Kashiyama^{1,2*}, Naoki. Seto³

¹*Department of Physics and Center for Particle Astrophysics, Pennsylvania State University, University Park, PA, 16802*

²*Department of Astronomy & Astrophysics, Pennsylvania State University, University Park, PA, 16802*

³*Department of Physics, Kyoto University, Kyoto 606-8502, Japan*

Accepted 2012 August 14. Received 2012 June 14

ABSTRACT

We investigate the capability of pulsar timing arrays (PTAs) as a probe of primordial black holes (PBHs), which might constitute the Galactic dark matter. A PBH passing nearby the Earth or a pulsar gives an impulse acceleration and induces residuals on otherwise orderly pulsar timing data. We show that the timing residuals induced at pulsars are optimal for searching heavier PBHs than those at the Earth, and the two probes are highly complementary. Future facilities like SKA could detect PBHs with masses around $\sim 10^{22-28}$ g even if only a small fraction ($\lesssim 1\%$) of the Galactic dark matter consists of these PBHs.

Key words: pulsars: general - cosmology: dark matter

1 INTRODUCTION

A significant fraction of matter in our Galaxy is considered to be occupied by dark matter, but its nature is poorly understood at present (Bertone, Hooper, & Silk 2005). Primordial black holes (PBHs) are an interesting astrophysical candidate of dark matter, and various observational constraints have been posed on their allowed mass range (Carr et al. 2010; Khlopov 2010). However, the current constraints in the mass range 10^{20} g $< M_{\text{PBH}} < 10^{27}$ g remain relatively weak.

To examine PBHs in this range, Seto & Cooray (2007) proposed an observational technique to directly probe gravitational interaction between the solar system and a nearby PBH. Around their close approach, the Earth receives an impulse of acceleration whose profile depends on the mass, distance, and velocity of the PBH. Given the local mass density of dark matter, the expected magnitude of the acceleration is very small, but high-precision measurements of pulsar timing could allow us to detect the weak impulse signal (see also Seto & Cooray (2004); Saito & Yokoyama (2009); Griest et al. (2011)).

Roughly speaking, in the present context, the pulsar timing analysis can be essentially regarded as measurement of the arrival times of radio pulses that were emitted by a pulsar and received on the Earth. The local accelerations of both of the pulsar and the Earth are encoded in the modulation of the time-of-arrival (TOA) data, as a simple linear combination of two separate terms for the two masses. We

call them by the pulsar term and the Earth term respectively.

When observing multiple pulsars for PBH search, the Earth terms are commonly excited by the acceleration of the Earth, and have coherent structure among TOA data of different pulsars. Therefore, we can statistically amplify the weak impulse signature on the Earth by using a pulsar timing array (PTA) and effectively reducing the timing noises. The underlying statistical approach here is similar to that for detecting gravitational waves (GWs) whose effect on the TOA data can be also expressed with two terms induced separately at the pulsar and the Earth (Sazhin 1978; Detweiler 1979; Hellings & Downs 1983). For the GW signals, we call them by the pulsar GW term and the Earth GW term, in order to distinguish them from the two acceleration terms. The traditional target of PTAs is the Earth GW terms.

Recently, it has been actively discussed that we might utilize the pulsar GW terms for analyzing GW sources such as merging super-massive black hole binaries (Jenet et al. 2004; Corbin & Cornish 2010; Lee et al. 2011; Ellis, Jenet, & McLaughlin 2012). To this end, we need sufficiently stable millisecond pulsars (MSPs), and such preferred systems might be discovered with future observational facilities. With the pulsar GW terms and known distances to the individual pulsars, our information content on GWs at the nano-Hertz band can be greatly increased, compared with that extracted from the Earth GW terms alone.

Meanwhile, if the timing noises of individual pulsars are small, we can also probe PBHs around the pulsars through the pulsar (acceleration) terms, in addition to PBHs close to the solar system. Then, the pulsar terms can largely widen

* E-mail: kzk15@psu.edu

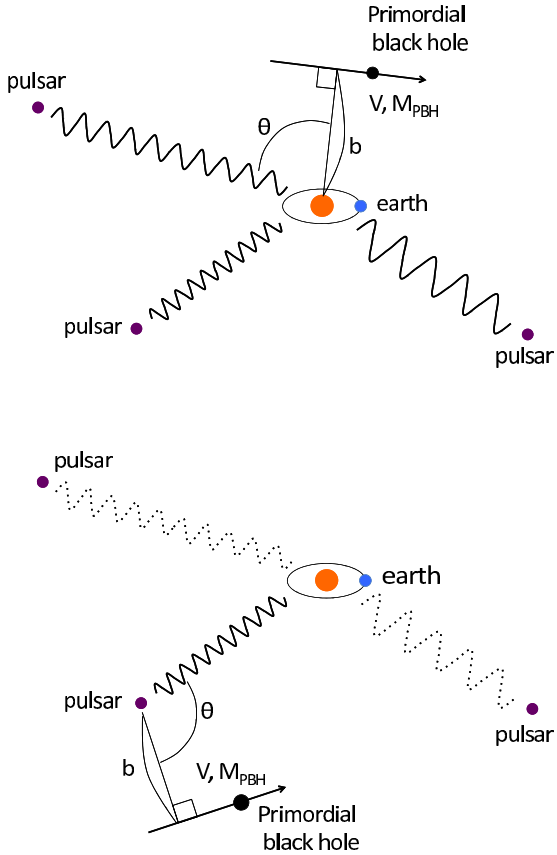


Figure 1. Schematic pictures of primordial black hole (PBH) searches using a pulsar timing array (PTA). The impulse signal of a PBH is characterized by its mass M_{PBH} , the relative velocity V to the target, the impact parameter b , and the projection angle θ between the pulsar-Earth line and the closest approach. *Top* panel shows the case with a PBH passing nearby the Earth. The acceleration by the PBH is imprinted in all the timing data available. By taking the correlation of the timing data, the signal can be effectively amplified by a factor of $\sqrt{N_{\text{PSR}}}$. *Bottom* panel shows the case with a PBH passing near a pulsar. The PBH modulates the timing data of the specific pulsar alone. The rate of such encounter is proportional to the number of pulsars N_{PSR} .

our survey volume, and our sensitivity for the direct PBH search would become better than the previous estimation only with the Earth terms (Seto & Cooray 2007). In this paper, we study this issue with special attention to the differences between the roles of two terms for the PBH search with PTAs, namely, the independent and numerous pulsar terms and the coherent Earth terms. We find that these terms have both advantages and disadvantages for PBH search, and work in a complementary way.

2 PROBING PRIMORDIAL BLACK HOLES USING PULSAR TIMING ARRAY

In this paper, we assume that our PTAs are composed by totally N_{PSR} pulsars with roughly the same level of timing noises. We further assume that the noises are white and have no correlation between different pulsars (see

Shannon & Cordes (2010) for impacts of red noises). Note that the total numbers of the Earth terms and the pulsar terms are both N_{PSR} .

In Fig.1, we provide schematic pictures of PBH search with a PTA. The top panel shows the case in which a PBH passes nearby the solar system and excites the Earth terms coherently for the TOA data of all the pulsars. In the bottom panel a PBH flybys a pulsar and modulates only the specific pulsar term.

As mentioned earlier, we can amplify the sensitivity of the Earth terms by a factor of $\sim 1/\sqrt{N_{\text{PSR}}}$ using their coherent structure. In contrast, the flybys of PBHs around the whole pulsars occur $\sim N_{\text{PSR}}$ times more frequently than those around the Earth alone.

We hereafter assume that, when a PTA is available, the coherent Earth term can be removed from TOA data of each pulsar, and its pulsar term can be analyzed separately.

2.1 Signal to noise ratio

Here we estimate the signal-to-noise ratio (S/N) of a flyby event in the TOA data of a PTA. The target mass can be the Earth or one of the pulsars. In the Fourier space, the main contribution of the impulse acceleration is the mode with the frequency $f = 1/T$, where T is the time scale for the PBH passing around the target. In the same manner, the amplitude s_f of the mode can be estimated as $s_f \approx (aT^2/c) \times |\cos \theta|$. Here a is the peak magnitude of acceleration and θ is the angle between the pulsar-Earth line and the closest approach (see Fig.1). With the impact parameter b and the relative velocity V , the two quantities T and a are given as

$$T \approx \frac{b}{V} \sim 10\text{yr} \left(\frac{b}{740\text{AU}} \right) \left(\frac{V}{350\text{km/s}} \right)^{-1}, \quad (1)$$

and $a \approx GM_{\text{PBH}}/b^2$, where M_{PBH} is the mass of the PBH. Then the Fourier amplitude of the timing residual is expressed as $s_f \approx (GM_{\text{PBH}}/cV^2) \times |\cos \theta|$, or

$$s_f \sim 10\text{ns} \left(\frac{M_{\text{PBH}}}{10^{25}\text{g}} \right) \left(\frac{V}{350\text{km/s}} \right)^{-2} \left(\frac{|\cos \theta|}{0.58} \right). \quad (2)$$

Next we evaluate the noise associated with the timing analysis. Using the sampling rate ν of TOAs and the rms noise σ of each TOA, the Fourier mode of the timing noise at the frequency $f = 1/T$ is given as $\sim \sigma/\sqrt{T\nu}$. This result is for TOA data of a single pulsar. When we deal with a PTA, it is important to distinguish whether we examine the Earth terms or a pulsar term. For the former, we have the statistical reduction factor $1/\sqrt{N_{\text{PSR}}}$ from the coherence of the signals. Therefore, the effective noise level for the impulse search can be expressed as

$$n_f \sim 6.2\text{ns} \left(\frac{\sigma}{100\text{ns}} \right) \left(\frac{T}{10\text{yr}} \right)^{-1/2} \left(\frac{\nu}{0.50\text{wk}^{-1}} \right)^{-1/2} N_{\text{PSR}}^{-E/2} \quad (3)$$

with $E = 0$ or 1 for a pulsar term and the Earth terms, respectively. From Eqs.(2) and (3) the signal-to-noise ratio of the flyby detection is now given as $S/N \equiv s_f/n_f$.

The signal of PBH is observationally characterized by the duration T and the amplitude s_f . On the other hand,

there are four physical parameters, b , M_{PBH} , V , and θ .¹ Thus, in general, we can obtain only two constraints between these four parameters, even if the signal is detected with a high signal-to-noise ratio. However, when constraining the parameters of PBHs as a dominant component of dark matter, we can set fiducial values for V and θ based on the following considerations. The rms velocity for halo dark matter relative to the solar system is dynamically estimated to be $\sim 350\text{km/s}$ (Carr & Sakellariadou 1999). Besides, the typical peculiar velocity of the observed MSPs are relatively small $\lesssim 100\text{km/s}$ (Hobbs et al. 2005). Thus, it is reasonable to fix $V = 350\text{km/s}$ for discussing both the Earth and pulsar terms induced by PBHs. Furthermore, if the scatterings between PBHs and the targets occur isotropically, the ensemble average of the projection angle θ becomes $\sqrt{\langle \cos^2 \theta \rangle} = 1/\sqrt{3} \sim 0.58$. Hereafter we fix $|\cos \theta| = 0.58$ as the fiducial value. Now the observational parameters (T and s_f) and the physical parameters (b and M_{PBH}) have one-to-one correspondence in our order-of-magnitude estimation.²

2.2 Event rate

The density of the local dark matter is estimated to be $\rho_{\text{DM}} = 0.011 M_{\odot} \text{pc}^{-3}$ (Olling & Merrifield (2001), see also Moni Bidin et al. (2012) for a recent claim). We put η as the mass fraction of PBHs among the Galactic dark matter, and assume that the PBHs have an identical mass parameterized by M_{PBH} . Then we can estimate the event rate of the close encounter of a PBH around the target masses within a impact parameter b as $R \approx \pi b^2 V \times (\rho_{\text{PBH}}/M_{\text{PBH}}) \times N_{\text{PSR}}^{1-E}$, or

$$R \sim 0.032 \text{yr}^{-1} \left(\frac{\eta}{1}\right) \left(\frac{\rho_{\text{DM}}}{0.011 M_{\odot} \text{pc}^{-3}}\right) \left(\frac{M_{\text{PBH}}}{10^{25} \text{g}}\right)^{-1} \times \left(\frac{b}{740 \text{AU}}\right)^2 \left(\frac{V}{350 \text{km/s}}\right) N_{\text{PSR}}^{1-E}. \quad (4)$$

We take $E = 0$ or 1 depending on whether a PBH flybys one of the pulsars ($E = 0$) or the Earth ($E = 1$). The factor N_{PSR}^{1-E} reflects the fact that, only in the case of using the independent pulsar terms, the event rate is proportional to the number of pulsars.

2.3 Detectable parameter regions

Now we discuss the observational prospects of PBH search. To this end, we examine the detectable PBHs in the two dimensional space (M_{PBH}, b) , assuming two future PTAs whose basic parameters are summarized in Table.1. PTAa has a relatively conservative set of parameters, and could be realized in the near future (Ellis, Jenet, & McLaughlin 2012). The goal of PTAb is more challenging and might

¹ For a PBH passing around the Earth, we can, in principle, estimate the direction of its closest approach, using the dipole pattern of the Earth terms in a PTA.

² We should note that some of the observed MSPs have comparable or larger peculiar velocities (*e.g.* B1957+20 Hobbs et al. (2005)). Also the scattering between PBHs and the targets may occur in a non-isotropic way, in which $\sqrt{\langle \cos^2 \theta \rangle}$ takes a different value. We discuss these cases in the final section.

Table 1. Parameter sets of the two pulsar timing arrays assumed for future prospects of PBH searches

	PTAa	PTAb
timing noise in each TOA (σ)	100ns	10ns
frequency of TOA sampling (ν)	0.5wk^{-1}	1.0wk^{-1}
number of pulsars (N_{PSR})	100	1000
observation time (T_{obs})	10yr	20yr

be realized with future facilities like SKA (*e.g.* Smits et al. (2011)). The latter will also enable us to estimate the parallax distances to the stable pulsars with typical errors of $\lesssim 20\%$. Then we can obtain broad scientific results, including a map of the interstellar electron density (Smits et al. 2011).

For detecting a PBH, we request that the following three conditions are simultaneously satisfied in the (M_{PBH}, b) -plane;

- (i) S/N is larger than a threshold value (*e.g.* $S/N > 3$ for 99% confidence level).
- (ii) At least one event occurs during the observation time ($R \times T_{\text{obs}} > 1$).
- (iii) The duration of signal is shorter than the observation time ($T < T_{\text{obs}}$).

From Eqs.(2) and (3), the condition (i) corresponds to the region in the (M_{PBH}, b) -plane as

$$\begin{aligned} \left(\frac{M_{\text{PBH}}}{10^{25} \text{g}}\right) \left(\frac{b}{740 \text{AU}}\right)^{1/2} &\gtrsim 0.56 \left(\frac{\sigma}{100 \text{ns}}\right) \left(\frac{\nu}{0.5 \text{wk}^{-1}}\right)^{-1/2} \\ &\times \left(\frac{V}{350 \text{km/s}}\right)^{5/2} \left(\frac{|\cos \theta|}{0.58}\right)^{-1} \\ &\times \left(\frac{S/N}{3}\right) N_{\text{PSR}}^{-E/2}. \end{aligned} \quad (5)$$

By reducing the rms noise σ , the overall sensitivity is improved and smaller PBHs are within reach. With the Earth terms, the detectable PBH mass becomes $1/\sqrt{N_{\text{PSR}}}$ time smaller than the limit with a pulsar term.

From Eq.(4), the condition (ii) can be expressed as

$$\begin{aligned} \left(\frac{M_{\text{PBH}}}{10^{25} \text{g}}\right) \left(\frac{b}{740 \text{AU}}\right)^{-2} &\lesssim 0.32 \left(\frac{\eta}{1}\right) \left(\frac{\rho_{\text{DM}}}{0.011 M_{\odot} \text{pc}^{-3}}\right) \\ &\times \left(\frac{V}{350 \text{km/s}}\right) \left(\frac{T_{\text{obs}}}{10 \text{yr}}\right) \\ &\times N_{\text{PSR}}^{1-E}. \end{aligned} \quad (6)$$

When fixing the PBH fraction η , the event rate scales as $R \propto M_{\text{PBH}}^{-1}$, and PBHs encounter the individual target masses less frequently for larger M_{PBH} . On the other hand, the event rate is also proportional to the number of the target masses. Thus, rare encounters with massive PBHs can be probed with the pulsar terms.

From Eq.(1), the condition (iii) for the signal duration can be expressed as

$$b \lesssim b_{\text{max}} = 740 \text{AU} \left(\frac{T_{\text{obs}}}{10 \text{yr}}\right) \left(\frac{V}{350 \text{km/s}}\right)^{-1}. \quad (7)$$

When we fix the relative velocity, the signal duration T has the one-to-one correspondence to the impact parameter $b(\equiv VT)$. The observation time limits the duration of the detectable signal, and so does the impact parameter.

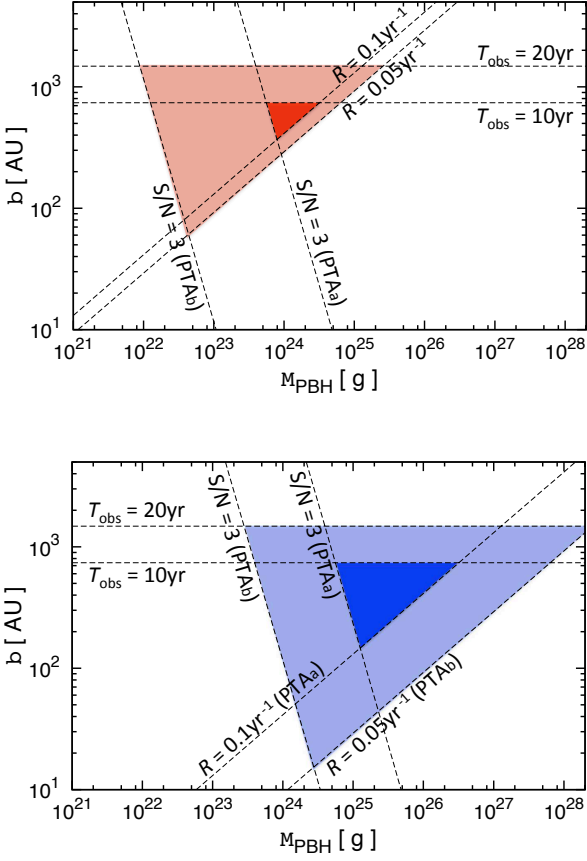


Figure 2. Detectable parameter regions of a primordial black hole (PBH) with mass M_{PBH} passing nearby the Earth (top panel) or a pulsar (bottom panel) with impact parameter b . The dark-colored regions correspond to the detectable events by PTAA, and the light-colored ones for PTAb (see Table.1). Here we fix the relative velocity of PBHs at $V = 350\text{km/s}$, and the projection factor at $|\cos\theta| = 0.58$. We assume that the dark matter density is $\rho_{\text{DM}} = 0.011M_{\odot}\text{pc}^{-3}$ with the PBH fraction $\eta = 1$. The lines with the slopes $b \propto M_{\text{PBH}}^{-2}$, $b \propto M_{\text{PBH}}^{1/2}$, and $b = \text{const}$ correspond to the conditions (i), (ii) and (ii) in the main text, respectively.

Fig.2 shows detectable parameter regions of a PBH in the (M_{PBH}, b) -plane for $\eta = 1$. The top panel is for a PBH passing near the Earth, and the bottom one is for those near the pulsars. In each panel, the dark-colored regions represent the detectable events with PTAA, and the light-colored ones are for PTAb.

In Fig.2, the lines with $b \propto M_{\text{PBH}}^{-2}$, $b \propto M_{\text{PBH}}^{1/2}$, and $b = \text{const}$ correspond to the conditions (i), (ii) and (iii), respectively (see Eqs.(5), (6) and (7)). As one can see easily from Fig.2, the Earth terms and the pulsar terms are highly complementary. The Earth terms cover a lighter mass range $\sim 10^{22-24}\text{g}$, compared with the range $\sim 10^{24-28}\text{g}$ probed by the pulsar terms.

Fig.3 shows possible constraints on the PBH fraction η with the two PTA models. Again, the top (bottom) panel shows the case using the Earth (pulsar) terms. The detectable region is bounded by two lines. The condition $S/N > 3$ sets the minimum mass of detectable PBH with the

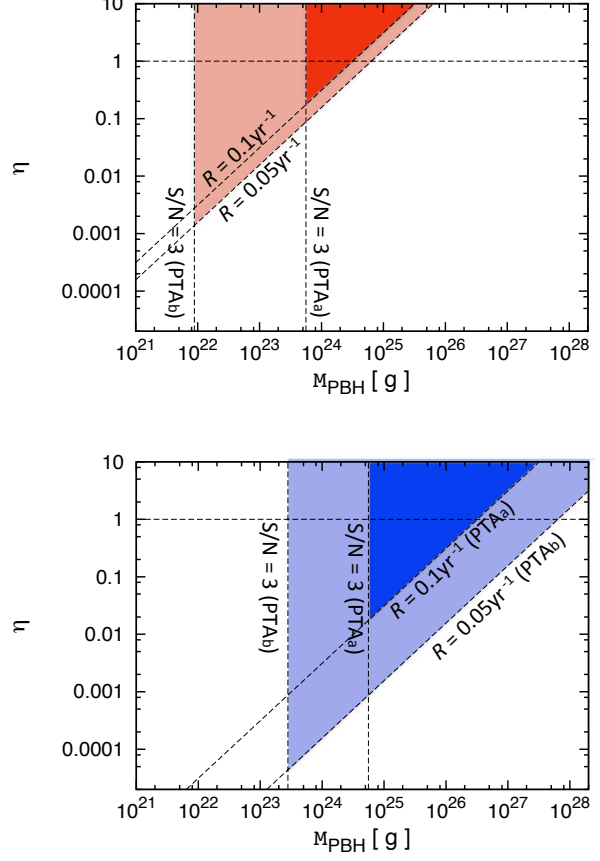


Figure 3. Possible constraints on the primordial black hole (PBH) abundance ($\eta \equiv \rho_{\text{PBH}}/\rho_{\text{DM}}$) using the two PTAs (the dark-colored regions for PTAA, and the light ones for PTAb). As in Fig.2, the top (bottom) panel shows the case with the Earth (pulsar) terms. We put $V = 350\text{km/s}$, $|\cos\theta| = 0.58$, and $\rho_{\text{DM}} = 0.011M_{\odot}\text{pc}^{-3}$. The lines with the slopes $M_{\text{PBH}} = \text{const}$, and $\eta \propto M_{\text{PBH}}$ correspond to the conditions (i) and (ii) respectively, with the impact parameter at b_{max} .

line $M_{\text{PBH}} = \text{const}$ (see Eq.(5)), and event rate determines the maximum one with $\eta \propto M_{\text{PBH}}$ (Eq.(6)). These boundaries can be understood in the following manner. For a given observational period T_{obs} , the impact parameter takes the upper limit $b_{\text{max}} = VT_{\text{obs}}$ given in Eq.(7). Next, when the PBH mass M_{PBH} is fixed, the signal-to-noise ratio and the sensitivity to the ratio η both take their optimal values at $b = b_{\text{max}}$, as shown in Eqs.(5) and (6).

If no event is detected by the PTAA observation, PBH with 10^{24}g to 10^{26}g is excluded as a dominant component of dark matter ($\eta \lesssim 0.1$). Moreover, in the case of the PTAb observation, PBH within 10^{22-28}g could be excluded ($\eta \lesssim 0.01$).

3 DISCUSSIONS

Our order-of-magnitude estimation has shown that we might probe PBHs or constrain their abundance with future PTAs. Here let us discuss issues related to the PBH search.

3.1 Data analysis and competing noises

So far we have simply evaluated the signal-to-noise ratios of fly-by events, assuming white noise spectra for timing noises of MSPs. But we should pay much attention to whether PBH signals can be clearly identified in their TOA data.

The actual timing analysis typically proceeds as follows (see *e.g.* Hobbs, Edwards, & Manchester (2006); Edwards, Hobbs, & Manchester (2006) for the detail). First, the measured TOAs are converted to the pulse emission times in the presumed reference frame of each MSP. In this step, various effects are estimated, such as the propagation delays, the ephemerides, and the coordinate transformation from the Earth to the pulsar. The derived time of emission is fitted by a timing model including a pulse frequency and its time derivative. The residual is divided into a white noise and un-modeled systematic noises which could include the signal we are seeking. A key in our approach to enlarge the detectable range of PBH mass is to consult both the coherent Earth terms and the individual pulsar terms. These two are assumed to be separated.

Here, we should be aware of the risk to mistake PBH signals for other effects while processing the TOA data, which could also lead to misestimation of the parameters of each pulsar. To prevent this, more detailed modeling of the PBH signal is required.

With a PTA, we have a large number of independent pulsar terms. The impulse accelerations by fly-by PBHs appear in the pulsar terms as sparse and isolated signals with finite durations. Therefore, a long-term observational campaign would be quite helpful to select sufficiently stable MSPs and examine the characteristic time profiles of the PBH signals.

As mentioned above, we have assumed that the ordinary timing noise in each TOA is white, $\sigma_{\text{WN}} \propto T^0$ (T : the observational time span). As for non-recycled pulsars, there have been confirmed secular red noises, $\sigma_{\text{RN}} \propto T^{2 \pm 0.2}$ (Shannon & Cordes 2010). Although most of the observed MSPs only have upper limits on the amplitude of the red noise, it might be identified by future PTAs to be obstacle in the PBH search.

3.2 Competing signals

Once a higher sensitivity as we have considered is realized, other possible signals also have to be opened up for discussion. They can be effective noises for PBH search and vice versa.

The most promising target of future PTAs is the GW background from merging supermassive black holes. The typical magnitude of the estimated dimensionless strain is $h \sim 10^{-15.5} \times (f/0.1\text{yr}^{-1})^{-2/3}$ (Jaffe & Backer 2003; Wyithe & Loeb 2003). This corresponds to the amplitude of the timing residual of $s_{f,\text{GW}} \sim 4.1\text{ns} \times (f/0.1\text{yr}^{-1})^{-5/3}$ (for the translation from h to $s_{f,\text{GW}}$, see *e.g.* Hobbs et al. (2009)), which can be comparable to that induced by PBHs (see Eq.(2)). Given the effective sensitivities of the pulsar and the Earth terms, the latter would be more vulnerable to the existence of the GW background. But, using the angular patterns of the Earth terms, we can, in principle, separate the two competing signals, as follows (Seto & Cooray 2007). A PBH signature in the Earth terms will have a dipole

pattern ($l = 1$) whose direction is determined by the acceleration vector. On the other hand, the GW background will have multiple modes starting from the quadrupole ($l = 2$).

One may suspect that floating planets (Sumi et al. 2011) could also become an effective noise because of the similar masses to PBHs we are interested in. There are expected to be a few times more floating planets than stars. The anticipated encounter rate with a pulsar is $\sim 10^{-(7-8)}\text{yr}^{-1} \times (b/740\text{AU})^2$, which is much smaller than PBH constituting a dominant fraction of dark matter (see Eq.(4)). Thus, we conclude that floating planets would not be problematic for our approach.

3.3 Possible refinements

Finally let us discuss possible improvements for our estimation of the detectable region of the PBH parameters.

In Fig.2 and Fig.3, we have fixed $V = 350\text{km/s}$, $|\cos\theta| = 0.58$, and $\rho_{\text{DM}} = 0.011M_{\odot}\text{pc}^{-3}$. These values correspond to the observed rms velocity for halo dark matter relative to the solar system, the mean projection factor for isotropic scatterings, and the local dark matter density near the solar system, respectively. These treatments should be regarded as a zeroth order approximation, and we can refine the present analysis in a more realistic manner.

For example, while the motions of the MSPs would be typically close to the Galactic rotation, those of PBHs would be more isotropic. Then the mean values for the projection factor $\cos\theta$ and the relative velocity V would depend on the Galactic position of each target MSP. In addition, the densities of the PBHs and the MSPs would also depend on the Galactic position. These would affect the estimation of the event rate and the strategy for data analysis.

Future facilities like SKA could determine the distance of MSPs up to 13kpc with $\lesssim 20\%$ accuracy (Smits et al. 2011). Multiple detections using the pulsar terms could potentially give us more detailed informations of the PBHs, such as their density and velocity distributions in the whole Galaxy, which can not be reached only using the Earth terms.

ACKNOWLEDGMENTS

This work is supported in part by the JSPS fellowship for research abroad, the JSPS grants, Nos.20740151 and 24540269. KK thanks P. Mészáros for useful discussions.

REFERENCES

- Bertone G., Hooper D., Silk J., 2005, *PhR*, 405, 279
 Moni Bidin C., Carraro G., Mendez R. A., Smith R., 2012, arXiv, arXiv:1204.3924
 Carr B. J., Sakellariadou M., 1999, *ApJ*, 516, 195
 Carr B. J., Kohri K., Sendouda Y., Yokoyama J., 2010, *PhRvD*, 81, 104019
 Corbin V., Cornish N. J., 2010, arXiv, arXiv:1008.1782
 Detweiler S., 1979, *ApJ*, 234, 1100
 Edwards R. T., Hobbs G. B., Manchester R. N., 2006, *MNRAS*, 372, 1549
 Ellis J. A., Jenet F. A., McLaughlin M. A., 2012, arXiv, arXiv:1202.0808
 Griest K., Lehner M. J., Cieplak A. M., Jain B., 2011, *PhRvL*, 107, 231101
 Hellings R. W., Downs G. S., 1983, *ApJ*, 265, L39
 Hobbs G., Lorimer D. R., Lyne A. G., Kramer M., 2005, *MNRAS*, 360, 974
 Hobbs G., et al., 2009, *MNRAS*, 394, 1945
 Hobbs G. B., Edwards R. T., Manchester R. N., 2006, *MNRAS*, 369, 655
 Jaffe A. H., Backer D. C., 2003, *ApJ*, 583, 616
 Jenet F. A., Lommen A., Larson S. L., Wen L., 2004, *ApJ*, 606, 799
 Khlopov M. Y., 2010, *RAA*, 10, 495
 Cordes J. M., Kramer M., Lazio T. J. W., Stappers B. W., Backer D. C., Johnston S., 2004, *NewAR*, 48, 1413
 Lee K. J., Wex N., Kramer M., Stappers B. W., Bassa C. G., Janssen G. H., Karuppusamy R., Smits R., 2011, *MNRAS*, 414, 3251
 Olling R. P., Merrifield M. R., 2001, *MNRAS*, 326, 164
 Saito R., Yokoyama J., 2009, *PhRvL*, 102, 161101
 Sazhin M. V., 1978, *SvA*, 22, 36
 Seto N., Cooray A., 2004, *PhRvD*, 70, 063512
 Seto N., Cooray A., 2007, *ApJ*, 659, L33
 Shannon R. M., Cordes J. M., 2010, *ApJ*, 725, 1607
 Smits R., Tingay S. J., Wex N., Kramer M., Stappers B., 2011, *A&A*, 528, A108
 Sumi T., et al., 2011, *Natur*, 473, 349
 Wyithe J. S. B., Loeb A., 2003, *ApJ*, 590, 691

This paper has been typeset from a $\text{T}_{\text{E}}\text{X}/\text{L}^{\text{A}}\text{T}_{\text{E}}\text{X}$ file prepared by the author.